NASA CONTRACTOR REPORT

NASA CR-2288

NASA CR-2288

A MODEL OF WIND SHEAR AND TURBULENCE IN THE SURFACE BOUNDARY LAYER

by James K. Luers

Prepared by
THE UNIVERSITY OF DAYTON RESEARCH INSTITUTE
Dayton, Ohio 45469
for George C. Marshall Space Flight Center

NATIONAL AERONAUTICS AND SPACE ADMINISTRATION • WASHINGTON, D. C. • JULY 1973

1. REPORT NO.	2. GOVERNMENT ACCESSION NO.	3. RECIPIENT'S CATALOG NO.
NASA CR-2288		

4. TITLE AND SUBTITLE	5. REPORT DATE
A MODEL OF WIND SHEAR AND TURBULENCE IN THE SURFACE BOUNDARY LAYER	July 1973
	6. PERFORMING ORGANIZATION CODE M112
7. AUTHOR(S) James K. Luers	8. PERFORMING ORGANIZATION REPORT #
9. PERFORMING ORGANIZATION NAME AND ADDRESS University of Dayton Research Institute Dayton, Ohio 45469	10. WORK UNIT NO.
	11. CONTRACT OR GRANT NO. NAS8-26600
12. SPONSORING AGENCY NAME AND ADDRESS NASA Washington, D. C. 20546	13. TYPE OF REPORT & PERIOD COVERED Contractor Report
	14. SPONSORING AGENCY CODE

15. SUPPLEMENTARY NOTES

Prepared under the technical monitorship of the Aerospace Environment Division, Aero-Astrodynamics Laboratory, NASA-Marshall Space Flight Center.

16. ABSTRACT

A model of wind and turbulence has been described for the surface boundary layer. The wind structure in the surface layer is considered to be a function of the surface parameters, stability, and height. The surface parameters considered are Z_o, the surface roughness length; u*, the surface friction velocity; and d, the zero plane displacement height. The stability parameter, Z/L, where L is the Monin-Obukov stability length, describes the thermal effect on the wind profile. The logarithmic wind profile is used to describe the mean wind field in the neutral boundary layer, and a logarithmic profile with a stability defect is used to describe the stable and unstable atmospheric conditions. For the very stable conditions, the logarithmic wind law does not hold. Under this condition, the layers of the atmosphere become disconnected and large scale frontal motions are the predominate factor in defining the wind profile. Figures are presented which represent some typical wind profiles in the very stable condition. The Dryden spectral function was chosen to represent the statistical properties of turbulence. The parameters of the Dryden model, σ and L (scale length), are specified as functions of stability, height, and surface conditions for each component of turbulence. The interrelationship between the components of σ and L are constrained to satisfy a condition of local isotropy at large wave numbers.

17. KEY WORDS	18. DISTRIBUTION STATEMENT
Boundary layer, turbulence, wind shear, atmospheric stability, friction velocity, surface rougness	02

19. SECURITY CLASSIF. (of this report)	20. SECURITY CLASSIF. (of this page)	21. NO. OF PAGES	22. PRICE
Unclassified	Unclassified	42	$3.00

For sale by National Technical Information Service, Springfield, Virginia 22151

FOREWORD

The research reported in this document was motivated by the need for a definition of low level wind shear environments for use in studies relative to the effect of wind shears on aeronautical systems during the landing flight phase. Modeling the wind environment has received renewed interest in the last few years because of the commitment on the part of the aeronautical community to develop an all-weather automatic landing system. A wide variety of wind models has been proposed, each with its own merits and deficiencies, depending on the intended application. The model contained herein is an excellent contribution to this existing "stable" of models, and was developed for the assessment of the effects of wind shear on the landing flight phase of aeronautical systems. The user is cautioned against selecting a given model for a design or operational problem without examining the other available models.

This research was conducted by the University of Dayton Research Institute for the National Aeronautics and Space Administration, George C. Marshall Space Flight Center, Huntsville, Alabama, under the technical direction of Dr. George H. Fichtl of the Aerospace Environment Division. The support for this research was provided by Mr. John Enders of the Aeronautical Operating Systems Division, Office of Advanced Research and Technology, NASA Headquarters.

TABLE OF CONTENTS

LIST OF ILLUSTRATIONS

LIST OF SYMBOLS

A, B, C, D	Constants
d	Zero wind reference level
f	Non-dimensional frequency; f = Kz
f_{max}	Frequency where spectrum is a maximum
g	Gravitational acceleration
k	Von Karman constant
K	Wave number
L	Monin-Obukov stability length
L	Scale length of turbulence
Ri	Richardson number
Ri_c	Critical Richardson number
S	Non-dimensional shear
T	Temperature
$\bar{u}$	Mean wind velocity
u*	Surface friction velocity
u	Longitudinal component of wind
v	Lateral component of wind
w	Vertical component of wind
Z	Altitude above zero plane displacement level
Z_o	Surface roughness length
Z'	Altitude above surface
Z_L	Altitude of interface between winds of different velocities
Γ	Adiabatic lapse rate
γ	Temperature lapse rate
ρ	Correlation coefficient
σ	Standard deviation of gust velocity
Φ	Spectral density function
Φ_ϵ	Non-dimensional dissipation rate

INTRODUCTION

An accurate and detailed description of the wind and turbulence structure of the planetary boundary layer has many applications. For example, a knowledge of wind and turbulence properties can be used to determine flow patterns and atmospheric mixing properties for use in pollution control. In addition, Structural Engineers must now consider the response of large buildings to the wind field; this requires a vertical profile of the wind field. The following discussion concerns the aircraft landing problem, particularly with respect to STOL aircraft. The two components of this problem are (a) the wake effects of buildings around STOL ports, and (b) the effects of a sudden change in wind magnitude or direction during final approach. A vertical wind profile over and around the structure in conjunction with information about wakes behind buildings is needed as input in order to define the former effect. A study of the latter effect has resulted in the formulation of a structural model of wind and turbulence in a statistically stationary and horizontally homogeneous boundary layer which has been used as the wind input to simulated aircraft landings. By observing the deviation in touchdown point from a zero wind condition, the types of profiles that provide hazardous landing conditions can be analyzed.

GENERAL DISCUSSION

A model has been selected for the mean wind profile and for the spectral characterization of turbulence in the statistically stationary and horizontally homogeneous surface boundary layer. In the surface boundary layer, only (a) the surface conditions, (b) the stability conditions, and (c) altitude are considered to influence the wind structure. The horizontal

shearing stress is constant. The wind direction is considered constant with altitude. Inertial, Coriolis, and pressure gradient forces are not considered significant in the surface boundary layer. The surface layer, in a strict sense, extends to only about ten meters altitude, but the above surface layer assumptions are reasonable to an altitude of nearly 100 meters.

SUMMARY OF MEAN WIND MODEL

The mean wind profile that has been selected for the surface boundary layer is a function of the surface parameters, u* (surface friction velocity), Z_o (roughness length), and d (zero plane displacement); the stability parameter Z/L (L is the Monin-Obukov stability length); and the height, Z. The model defined by these parameters reasonably approximates the true wind profile to an altitude of 100 meters. A definition of the parameters u*, Z_o, d, Z/L, and a discussion of rationale pertinent to the selection of this model is presented in a later section.

The mean wind for the surface boundary layer is described by the Logarithmic law

$$\bar{u} = \frac{u^*}{k}\left[\ell n \left(\frac{Z + Z_o}{Z_o}\right) + \Psi\left(\frac{Z}{L}\right)\right] \quad ,$$

where, for neutral stability,

$$\Psi\left(\frac{Z}{L}\right) = 0;$$

for an unstable condition,

$$\Psi\left(\frac{Z}{L}\right) = \int_{Z_o/L}^{Z/L} \frac{L}{Z}\left\{1 - \left(1 - a\,\frac{Z}{L}\right)^{-1/4}\right\} d\left(\frac{Z}{L}\right),$$

with the parameter a = 18;

and for the stable condition,

$$\Psi\left(\frac{Z}{L}\right) = \alpha \frac{Z}{L}, \text{ with the parameter } \alpha = 5.2.$$

For the very stable condition, the logarithmic wind law does not hold. Under strong inversion conditions, the layers of the atmosphere become disconnected and large scale frontal motions are the predominate factor in defining the shape of the profile. Figures 5 and 6, shown and discussed later, define typical types of profiles that may occur in the very stable condition.

SUMMARY OF TURBULENCE SPECTRA

Deviations in wind velocity having periods of less than ten minutes are considered gusts or turbulence. The statistical properties of turbulence are characterized by its spectrum. For the aircraft landing simulation problem, the functional representation of the turbulence spectra has been chosen as the Dryden spectral function. The parameters of the Dryden spectra, σ_u, σ_v, σ_w, and L_u, L_v, L_w, have been defined as functions of stability, height, and surface conditions. The surface roughness parameter, Z_o, is not sufficient to explain the terrain effect on the components of σ and L. Large scale terrain features are important, but insufficient data has been collected to categorize their effect. A later section discusses the various sources of data which served as a basis for choosing this model.

The expression for the vertical velocity standard deviation is

$$\sigma_w = 1.25 u^* \left(1 - \frac{Z/L}{S}\right)^{1/4}$$

where

$$S = 1 + 5.2\frac{Z}{L} \quad \text{for} \quad \frac{Z}{L} \geq 0$$

and

$$S = (1 - 18\frac{Z}{L})^{-1/4} \quad \text{for} \quad \frac{Z}{L} \leq 0 \quad .$$

The longitudinal and lateral velocity standard deviations, σ_u and σ_v, are defined in terms of the stability parameter B by Figures 8 and 9, presented later, where

$$B = \frac{Ri\, S^2}{\ell n(\frac{Z}{Z_o}) - \Psi(\frac{Z}{L})} \quad .$$

The vertical scale length is defined by

$$L_w = \frac{0.74Z}{\Phi_\epsilon}$$

where

$$\Phi_\epsilon = 1 + 9\frac{Z}{L} \quad \text{for} \quad \frac{Z}{L} \geq 0$$

and $\Phi_\epsilon = (1 - 18\frac{Z}{L})^{-1/4} - \frac{Z}{L}$ for $\frac{Z}{L} \leq 0$.

The longitudinal and lateral scale lengths are derived from the local isotropic turbulence relationship

$$\frac{L_u}{\sigma_u^2} = \frac{2L_w}{\sigma_w^2} = \frac{2L_v}{\sigma_v^2} \quad .$$

The L_w and L_v defined by this relationship show generally good agreement with independently measured experimental data.

SURFACE BOUNDARY LAYER

The surface boundary layer is defined as that region of the atmosphere where the shearing stress is constant. The region extends, in a strict sense, from the surface to only about ten meters altitude, but is

considered to extend to nearly 100 meters. In the ten-meter to 100-meter layer, the decrease in stress with altitude is so small as to make the assumption of constant shear stress acceptable for engineering applications. In the surface boundary layer only the surface conditions,the stability condition, and altitude affect the wind and turbulence structure. The following sections discuss the parameters used to describe the surface and stability conditions.

Surface Conditions

The surface parameters used in defining both the mean wind velocity profile and the spectral properties of turbulence are the surface roughness length (Z_o), the zero wind reference level (d), and the surface friction velocity (u*). The roughness length Z_o is a parameter used to characterize the gross features of the terrain. It is most reliably estimated for uniform type terrains. When the terrain is nonuniform, the dissimilar features influence the wind profile in a manner that depends upon the distance from these features. Thus, a gross roughness parameter is not appropriate for estimating a wind profile if the profile reflects the effects of nonuniform terrain elements. Fichtl [1] gives some typical values of roughness length for various types of uniform terrains. (See Table 1.)

The zero plane reference level, d, is the altitude at which, for a given roughness length, the wind velocity extrapolates to zero. (See Figure 1.) For example, over forest type terrain where the average height of the trees may be 15 meters, the roughness length is $Z_o \simeq$ 0.5 meter. The profile above the trees can be represented as a logarithmic function of altitude. The zero plane displacement is determined by

TABLE I*

TYPICAL VALUES OF SURFACE ROUGHNESS LENGTH (Z_o) FOR VARIOUS TYPES OF SURFACES

Type of Surface	z_0 (m)
Mud flats, ice	$10^{-5} - 3 \cdot 10^{-5}$
Smooth sea	$2 \cdot 10^{-4} - 3 \cdot 10^{-4}$
Sand	$10^{-4} - 10^{-3}$
Snow surface	$10^{-3} - 6 \cdot 10^{-3}$
Mown grass (~ 0.01 m)	$10^{-3} - 10^{-2}$
Low grass, steppe	$10^{-2} - 4 \cdot 10^{-2}$
Fallow field	$2 \cdot 10^{-2} - 3 \cdot 10^{-2}$
High grass	$4 \cdot 10^{-2} - 10^{-1}$
Palmetto	$10^{-1} - 3 \cdot 10^{-1}$
Suburbia	1 - 2
City	1 - 4

*This table was taken from George H. Fichtl, Reference 1.

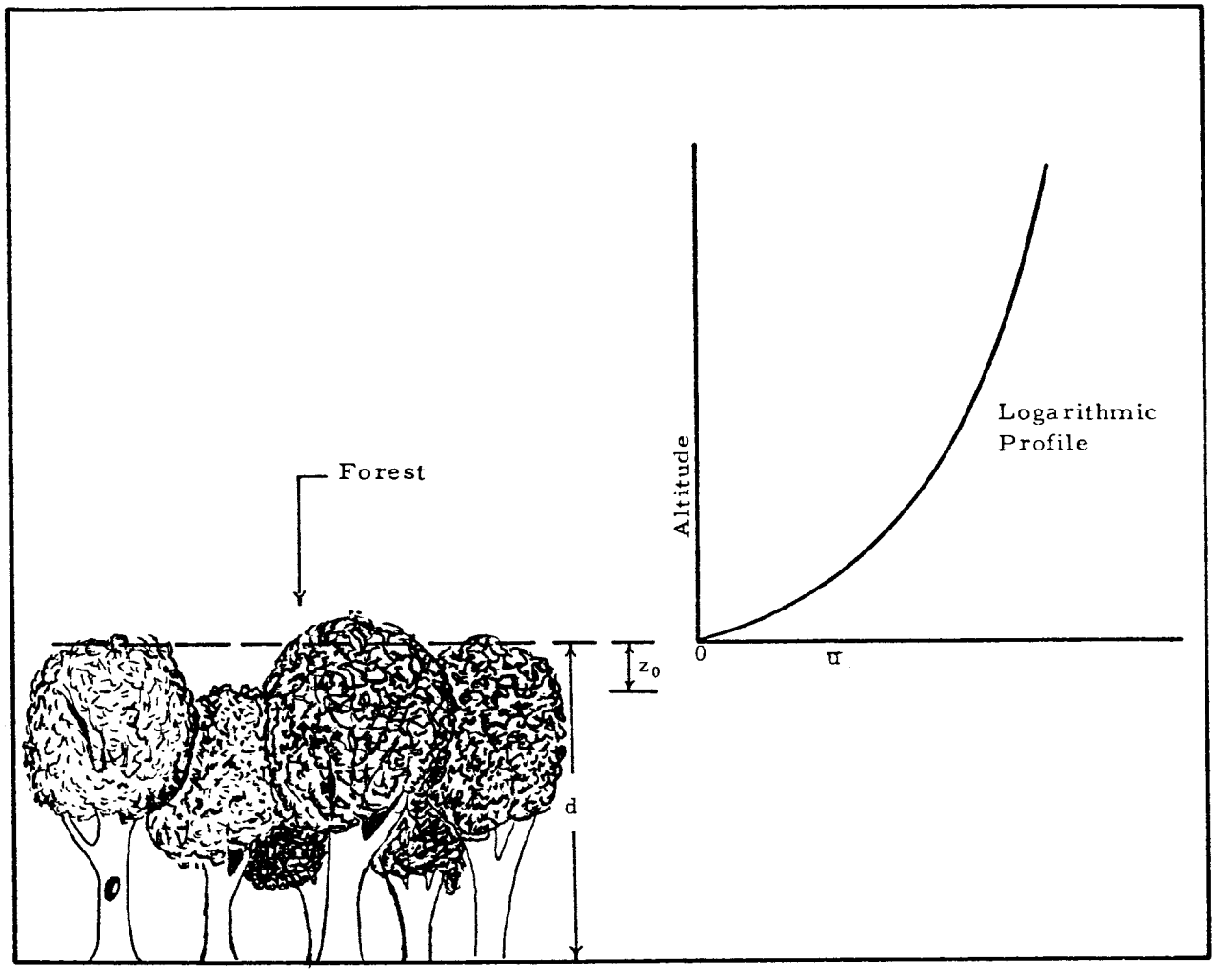

Figure 1. Logarithmic Wind Profile Above a Forest.

extrapolating the wind profile above the tree tops to the altitude at which the wind equals zero. In moderate wind fields, the zero plane displacement may be the approximate height of the roughness elements, in the above example, approximately 15 meters. In strong wind fields, the zero plane displacement tends to decrease while in light wind fields, it tends to increase. Thus, for an average guess, d can be taken as the average height of the roughness elements.

The surface frictional velocity u* is defined as $u^* = [-\overline{uw}]^{1/2}$, where $\overline{w}$ and $\overline{u}$ denote the vertical and longitudinal components of the fluctuating wind velocity, and overbar denotes a time average over approximately a ten-minute period. The fluctuating velocity is distinguished from the mean velocity by its duration. In practice, the mean wind is generally averaged over periods approximately equal to ten minutes and the fluctuating velocity is computed as deviations from the mean. Since a gap in spectral energy exists between approximately ten minutes and several hours, there should be little difference between an average computed over ten minutes and one over a one-hour period. [2] Thus, it is reasonable to define a fluctuating component of velocity as having a period less than ten minutes.

The frictional velocity is a scaling parameter for the mean wind profile. That is, the mean wind profile increases in direct proportion to the surface friction velocity. This can be seen as follows: The correlation coefficient, $\rho_{uw} = \overline{uw}/\sigma_u \sigma_w$, is assumed to be constant throughout the surface boundary layer (typically, $\rho_{uw} = -0.3$). Thus, $\overline{uw} = D\sigma_u \sigma_w$, $D = -0.3$, a constant for this discussion. In neutral stability σ_u and σ_w are known to vary proportional to the mean wind velocity. That is, $\sigma_u = A\overline{u}$ and $\sigma_w = B\overline{u}$. Thus, $u^* = [-\overline{uw}]^{1/2} = C\overline{u}$, where $C = \{DAB\}^{1/2}$.

Thus, in neutral stability, the mean wind is directly proportional to the surface friction velocity. In nonneutral stability, similarity theory again requires that $\bar{u}$ be directly proportional to u*.

Stability Parameters

The mean wind and turbulence in the surface layer depend upon the temperature profile. The temperature lapse rate, i.e., the decrease in temperature with altitude, measures the effect of the temperature profile on the wind velocity structure. If the decrease of temperature with altitude is greater than that associated with a homoentropic atmosphere (adiabatic lapse rate) then the temperature profile adds kinetic energy to the atmosphere via positive buoyancy forces. If, on the other hand, the temperature lapse rate is less than the adiabatic lapse rate, a downward restoring force absorbs energy from the atmosphere. In this case, the atmosphere is said to be stable. If the temperature lapse rate is approximately adiabatic, the atmosphere is neutral. Under strong inversion conditions, the damping effect becomes so prominent as to convert turbulent eddies into a laminar flow. This division between laminar and turbulent flow is generally defined by the critical Richardson number, Ri_c. For $Ri > Ri_c$, turbulence can no longer exist. This critical value is not accurately defined and may even be dependent on surface condition. An approximate value for the critical gradient Richardson number is $Ri \approx 0.20$ [2]. The expression for gradient Richardson number in terms of lapse rate and the adiabatic lapse rate is

$$Ri = \frac{g\,(\Gamma - \gamma)}{T\left(\frac{\partial \bar{u}}{\partial Z}\right)^2} \qquad (1)$$

where

g = gravitational acceleration,

Γ = adiabatic lapse rate = g/C_p,

γ = temperature lapse rate = $-\partial T/\partial Z$,

T = temperature,

C_p = specific heat of dry air at constant pressure,

$\bar{u}$ = mean wind velocity, and

Z = altitude.

Equation (1) shows that for neutral stability $Ri \approx 0$; for an unstable atmosphere $Ri < 0$; and for a stable atmosphere $Ri > 0$. The stable atmosphere is further subdivided by the critical Richardson number into stable for $Ri < Ri_c$ and very stable for $Ri > Ri_c$. In the very stable condition, when only laminar flow exists, the atmosphere becomes disconnected and the shape of the wind profile no longer reflects only the surface conditions. Large scale effects such as a warm front overrunning a cold front become the dominant features in shaping the profile. Physically, the Richardson number represents the ratio of the thermal to mechanical production of turbulence. For a statically stable atmosphere, $\Gamma > \gamma$, thermal damping occurs, and the Richardson number is positive. For an unstable atmosphere, $\gamma > \Gamma$, thermal convection adds energy to the atmosphere, and the Richardson number is negative. For a neutral atmosphere, there is essentially no thermal energy transferred and the Richardson number is approximately zero. The Richardson number has become an important and universally accepted measure of atmospheric stability. In defining wind profiles, however, the Richardson number is not easily manipulated because of its variability with altitude. A different parameter, Z/L, where L is the Monin-Obukov stability length, is a more convenient

stability parameter for characterizing wind profiles. The Monin-Obukov stability length can be considered independent of altitude in the surface layer and is defined by

$$L = \frac{u^{*3} C_p \rho \theta}{k g H}$$

where θ = potential temperature,

H = vertical heat flux,

ρ = air density, and

k = von Karman constant.

The parameter Z/L can be related to the Richardson number through dimensional analysis arguments and experiments show the relationship to be given by

$$Z/L = Ri \text{ for } Ri \leq 0 \text{ (Businger's hypothesis)}$$

and

$$Z/L = Ri/1-5.2\ Ri \text{ for } 0 < Ri < Ri_c.$$

The second expression above implies $Z/L \to \infty$ as $Ri \to 1/5.2$. This conforms to a critical Richardson number of approximately 0.20.

MEAN WIND PROFILE

In the surface boundary layer the logarithmic wind law as derived from the Monin-Obukov similarity theory and experiments for neutral ($Ri \simeq 0$), stable ($0 < Ri < Ri_c$), and unstable ($Ri < 0$) conditions is given by

$$\bar{u} = \frac{u^*}{k} \left[\ell n \left(\frac{Z' - d + Z_o}{Z_o} \right) + \Psi \left(\frac{Z' - d}{L} \right) \right], \qquad (2)$$

where the surface parameters u*, Z_o, and d, and the stability parameter, Z/L have been previously discussed. Z' is the height above the surface. The von Karman constant, k, has numerical value of approximately +0.4. Equation (2) can be written in the simplified form

$$\bar{u} = \frac{u^*}{k} \left[\ell n \left(\frac{Z + Z_o}{Z_o} \right) + \Psi \left(\frac{Z}{L} \right) \right] \qquad (3)$$

where Z is the altitude above the zero plane reference level. Equation (2) or (3) is useful only for fully turbulent boundary layers and does not provide a valid representation of the wind profile under very stable conditions.

The function $\Psi(Z/L)$ is an empirically derived universal function of Z/L. For neutral stability when Z/L = 0, $\Psi(0) = 0$, so that the log profile is valid, i.e.,

$$\bar{u} = \frac{u^*}{k} \ell n \left(\frac{Z + Z_o}{Z_o} \right) \quad .$$

Figure 2 shows neutral wind profiles for various values of u* and Z_o. The expression for $\Psi(Z/L)$ in unstable and stable air has been derived by many authors (Webb, Panofsky et al., McVehil, Fichtl and McVehil, Wyngaard and Cote, Businger et al., and others). [2, 3, 4, 5, 6, and 7]

For the unstable conditions $\Psi(Z/L)$ has been calculated by fitting the nondimensional shear $S = \frac{kZ\partial\bar{u}}{u^*\partial Z}$ to an equation of the form

$$S = (1 - a\,Ri)^{-1/4} \qquad (4)$$

where Ri = Z/L and a is a fitting parameter.

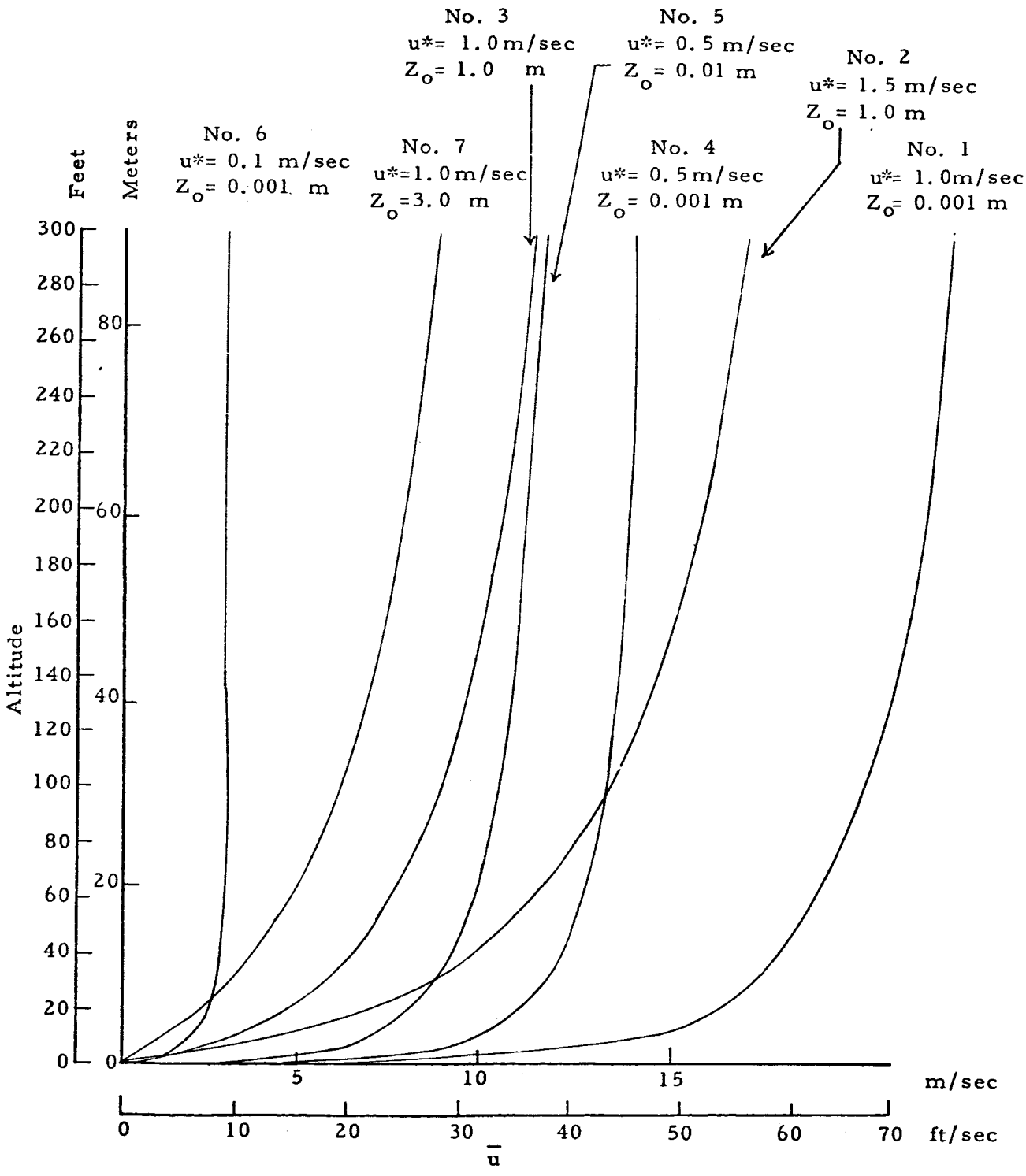

Figure 2. Neutral Wind Profiles.

Peterson and Panofsky [3] suggest a value of a = 18; Businger et al. suggest a = 15 with a von Karman k of 0.35. Integration of the nondimensional shear (Equation 4) defines the mean wind as

$$\bar{u} = \frac{u^*}{k}\left[\ell n\left(\frac{Z + Z_o}{Z_o}\right) + \Psi\left(\frac{Z}{L}\right)\right]$$

where

$$\Psi\left(\frac{Z}{L}\right) = \int_{Z_o/L}^{Z/L} \frac{L}{Z}\left\{1 - \left(1 - a\,\frac{Z}{L}\right)^{-1/4}\right\} \, d\,\frac{Z}{L} .$$

Figure 3 shows unstable wind profiles for various values of Z_o, u*, and L.

For a stable atmosphere, the nondimensional shear has been described by the expression

$$S = \frac{kZ}{u^*}\,\frac{\partial u}{\partial Z} = 1 + \alpha\,\frac{Z}{L} \qquad . \qquad (5)$$

Integration of Equation (5) with respect to altitude defines the mean wind profile for stable air as

$$\bar{u} = \frac{u^*}{k}\left[\ell n\left(\frac{Z + Z_o}{Z_o}\right) + \alpha\,\frac{Z}{L}\right] .$$

Peterson and Panofsky suggest a value for α of 10; Businger et al. suggest α = 4.5 to α = 5.0 with k = 0.35; McVehil suggests α = 7.0. Webb suggests α = 5.2 with individual observation showing a standard deviation of 30 percent from the mean value of 5.2. There is, in essence, some doubt as to whether the nondimensional shear is dependent only upon Z/L. For our wind shear model, the value of Webb, α = 5.2, has been selected. Figure 4 shows plots of stable wind profiles for various values of u*, Z_o, and L.

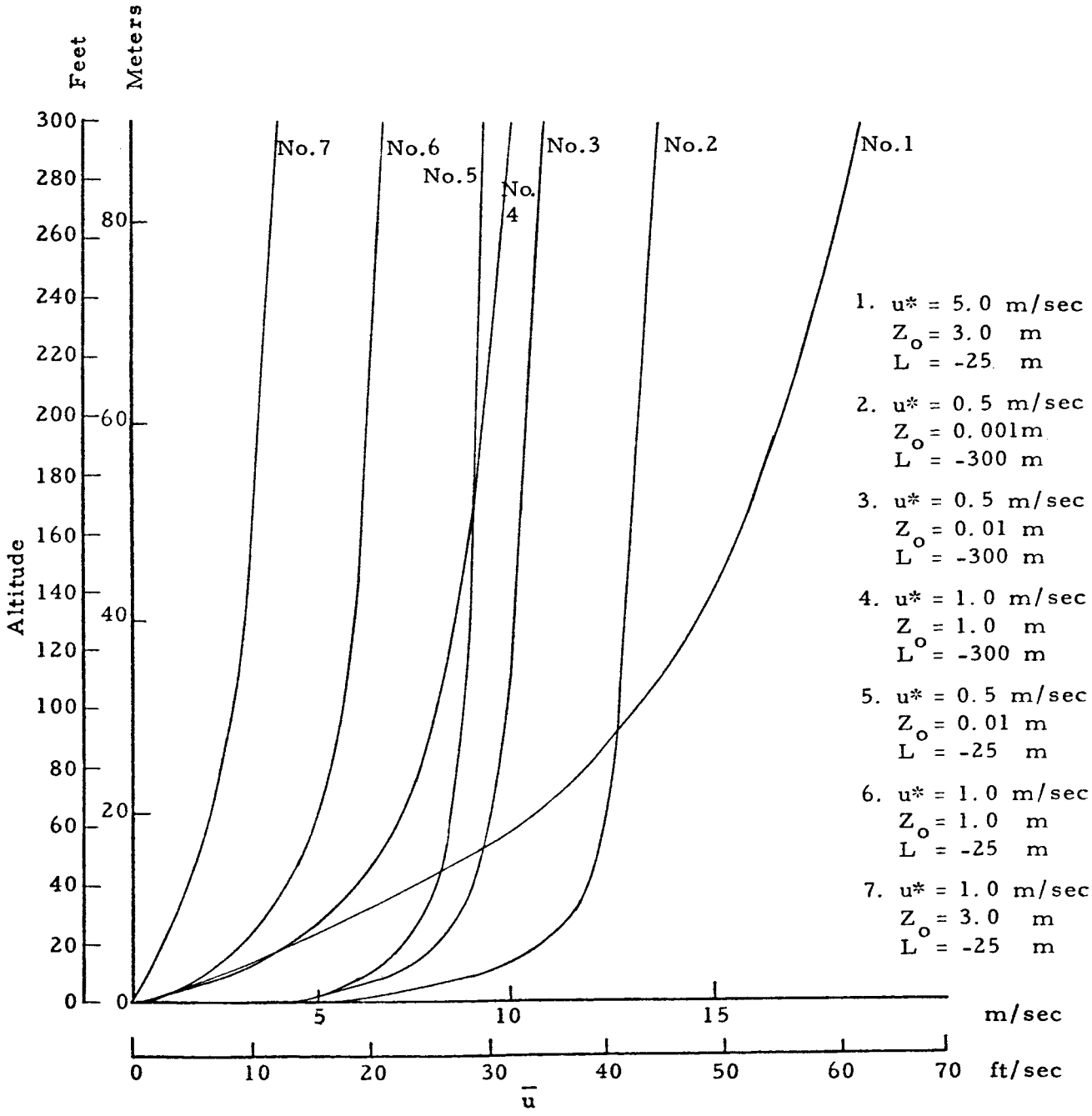

Figure 3. Unstable Wind Profiles.

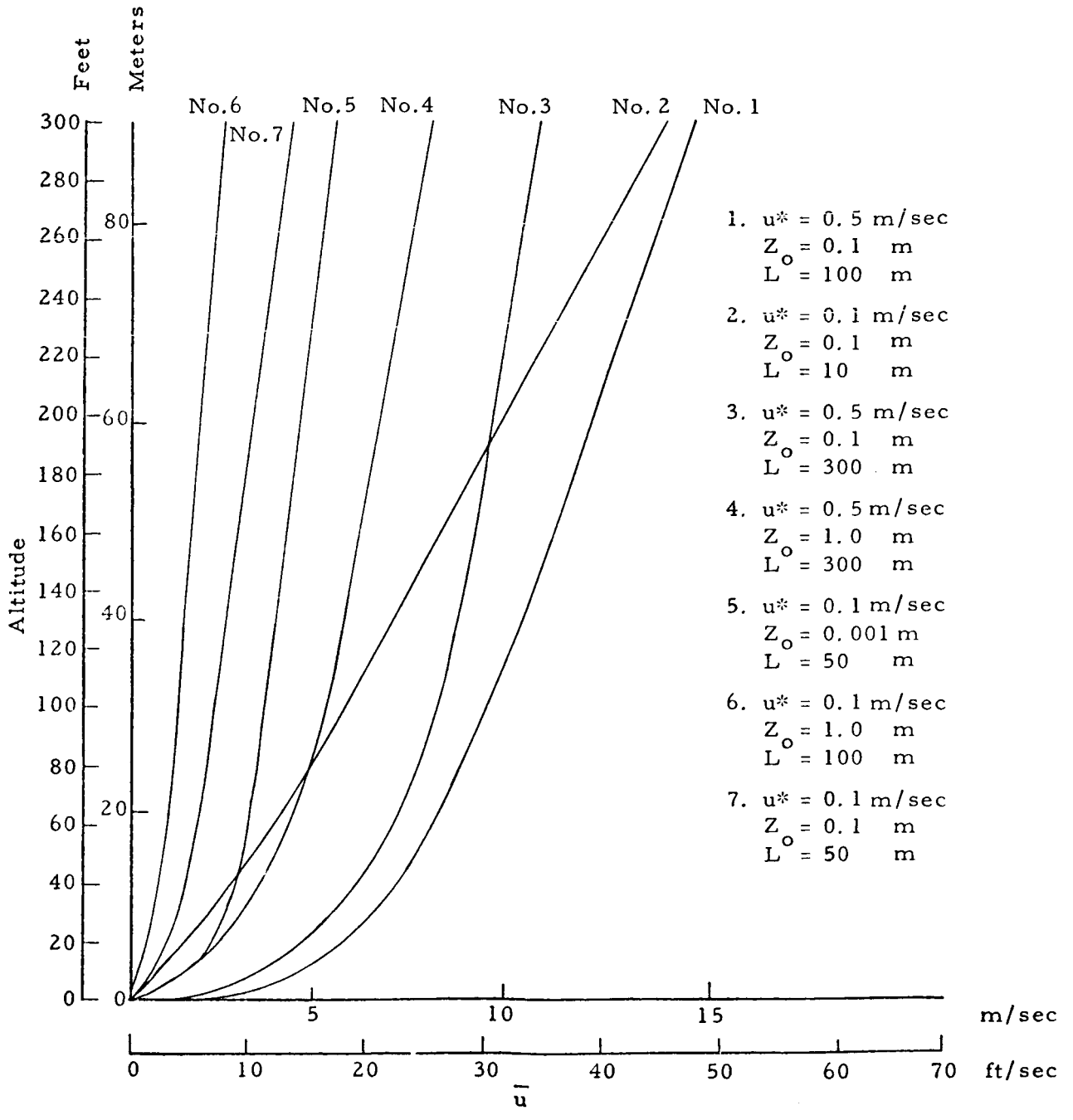

Figure 4. Stable Wind Profiles.

For the very stable conditions no analytic expression has been found to represent the wind profile. The shape of the profile is largely determined by large scale motions of a new air current overrunning a static front. Since the flow is laminar, very little mixing occurs and the overriding air remains separated from the underlying air. This condition also leads to the possibility of a large change in wind direction in the surface layer. Changes of wind direction in excess of 45 degrees are not uncommon in very stable air.[8] A few examples of the types of wind profiles that may occur are given in Figures 5 and 6. Figure 5 shows a calm below the interface level Z_L. Above the interface the wind is considered constant of magnitude $\bar{u}$, depending upon the velocity of the overriding air. $\bar{u}$ can be assumed constant above Z_L because the boundary effect produced by the earth's surface is not relevant and the boundary effect between nonmixing air masses of different velocities is negligible. Figure 5 also allows for a variation in the altitude Z_L where the interface occurs. Figure 6 shows a light wind condition which obeys the logarithmic wind law below the interface with a constant wind above the interface. This situation may occur when the atmosphere is in a neutral or stable condition below the interface. Large changes in wind direction are likely to occur with this type profile.

TURBULENCE SPECTRA

Measurements of deviations from the ten-minute to one-hour averaged mean wind are classified as turbulence or gusts. These gust measurements cannot be characterized in a deterministic sense and hence must be described statistically. The turbulence structure of the atmosphere is generally specified by its power spectra. Studies of

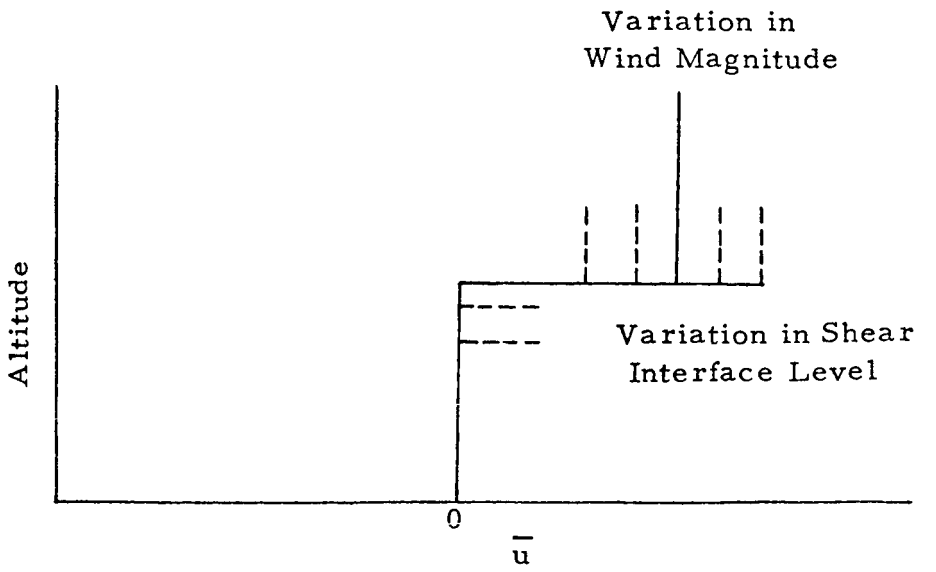

Figure 5. Very Stable Wind Profiles.

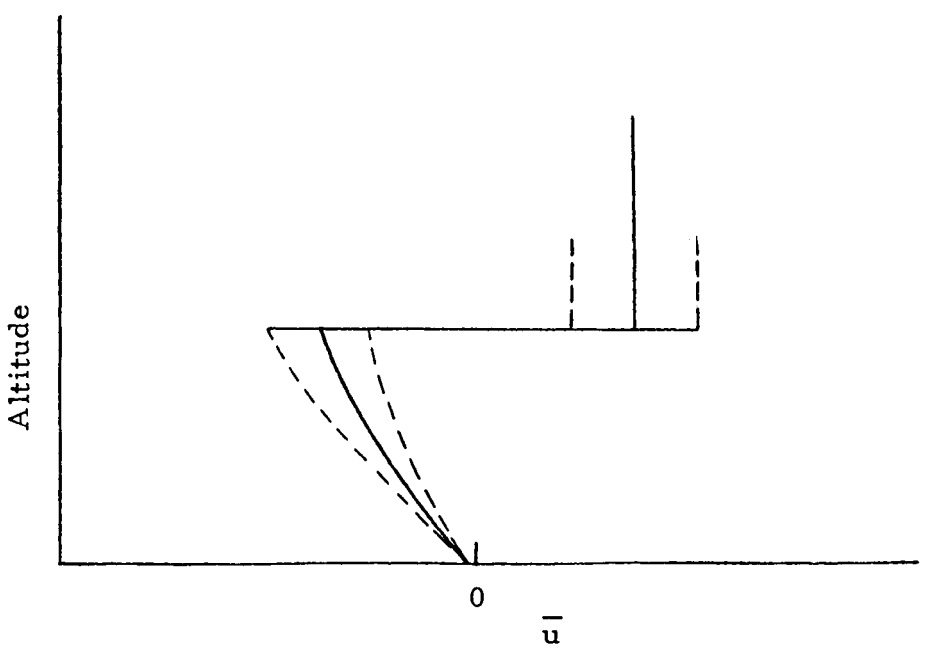

Figure 6. Very Stable Wind Profiles.

measured spectra have been fit to functions so that a functional representation of the spectra is possible. Some of the more prominent spectral density functions are the Dryden, von Karman, Busch-Panofsky, and Fichtl-McVehil spectral functions. The Dryden and von Karman functions are defined in terms of the parameters σ and L. Sigma is the standard deviation of the gust velocity and L is the integral scale length of turbulence defined as the integral of the correlation function. The Busch-Panofsky function is defined by the parameters σ and f_{max}, where f_{max} is the nondimensional frequency at which the spectrum takes on its maximum value. f_{max} is a function of stability only. The Fichtl-McVehil spectrum is a modification of the Busch-Panofsky spectrum which contains an additional parameter which is dependent upon height. Much of the data that has been collected has been fit by the Dryden and von Karman functions. From this data variation in σ and L with terrain, stability, and height has been analyzed. On only a relatively small percentage of the data has the variation in f_{max} with stability been examined. The von Karman spectrum differs from the Dryden spectrum primarily in the inertial subrange region. In this region local isotropy holds and there is essentially no production or dissipation of energy. The spectrum is proportional to the wave number, K, to the -5/3 power. Experimental data has largely substantiated the local isotropy and -5/3 slope hypothesis.

The von Karman function has the desirable property of being proportional to $K^{-5/3}$ in the inertial subrange. The Dryden function is proportional to K^{-2} in the inertial subrange. Thus, from this standpoint, the von Karman is the more desirable spectral density function.

For the aircraft landing problem, for which use of this model is intended, a digital simulation of turbulence is required. The von Karman

function, being an irrational function, is more difficult to simulate than the rational Dryden function. Furthermore, it has been shown by Flinn [9] that in observing aircraft response little difference can be seen between a Dryden and a von Karman input spectrum. Consequently, for the landing simulation problem, the Dryden spectrum has been chosen.

The parameters of the Dryden spectrum σ and L are functions of stability, surface conditions, and altitude. The standard deviation of a gust velocity time history from a running ten-minute to a one-hour mean is a common method used to measure σ. Consequently, the determination of σ is independent of the spectral density function being used (e.g., von Karman, Dryden, etc.). The same is not always true for the scale length parameter, L. The scale length L is often calculated by observing the wave number, K_{max}, at which the spectrum is a maximum and then relating K_{max} to L through the relationship

$$L_u = 0.146/K_{max}$$

and

$$L_v = 0.106/K_{max} = L_w \quad \text{for the von Karman spectrum,} \tag{6}$$

and

$$L_u = 0.159/K_{max}$$

and

$$L_v = 0.117/K_{max} = L_w \quad \text{for the Dryden spectrum.[10]} \tag{7}$$

Since Equations (6) and (7) are not identical, it follows that when fitting an experimental spectrum with the von Karman and Dryden functions, slightly different values of L would result. Percentagewise, however, the difference between the L values is small compared to the uncertainty

in defining K_{max}. Thus, for practical considerations, experimental values of L can be analyzed without regard to which spectral function was used to obtain L. If L values were obtained by an entirely different procedure such as by direct integration of the correlation function, they would be independent of the type of spectral function.

The following sections examine the stability, terrain, and height dependence of σ's and L's obtained from experimental measurements. As concluded in the above paragraph, the σ and L relationships are valid for use with both the Dryden and von Karman models.

Standard Deviation of Gust Velocities

Vertical Standard Deviation - Similarity theory predicts that the standard deviation of the vertical component of gust velocity normalized by the friction velocity depends only upon the stability parameter Z/L, i.e.,

$$\frac{\sigma_w}{u^*} = f\,(Z/L).$$

The function f as derived by Monin is

$$\frac{\sigma_w}{u^*} = c\left[\,1 - \frac{(Z/L)}{S}\right]^{1/4} \qquad (8)$$

where S is the nondimensional shear defined by Equations (4) and (5). Prasad and Panofsky [3] have shown Equation (8) to provide a good fit to experimental data when c = 1.25. This value of c implies that for the neutral stability condition

$$\frac{\sigma_w}{u^*} = 1.25,$$

a value that is in good agreement with what several other experimenters have observed in neutral stability. [3, 11, and 12] Other expressions can be found to represent the variation of σ_w with stability, most of which are in general agreement with Equation (8). Thus, Equation (8) will be used to define the standard deviation of the vertical gust velocity component. Figure 7 shows a plot of Equation (8).

Longitudinal Standard Deviation - The longitudinal component of gust, in contrast to the vertical component, has not been found to obey similarity theory. In particular, the ratio σ_u/u^* is not a function of stability only, but is also dependent upon large scale (hills, trees, buildings, etc.) surface terrain features. The surface roughness length, Z_o, does not appear sufficient to explain the variation in the ratio σ_u/u^* from one place to another in a given stability condition. The author is not aware of any study that has explained the terrain effect on σ_u/u^*. In neutral stability various measurements of the ratio have provided values between 2.1 and 2.9. [13, 14] The value of $\sigma_u/u^* = 2.5$ will be taken as an average value for this model in neutral stability.

The variation of the ratio σ_u/u^* with stability and height has been analyzed by Prasad and Panofsky [3] by introducing the stability parameter B defined as

$$B = \left(\frac{g}{T}\right)\left(\frac{Z^2}{\bar{u}Z}\right)(\Gamma - \gamma) \quad .$$

B is related to Z/L, Z_o, and Z through the expression

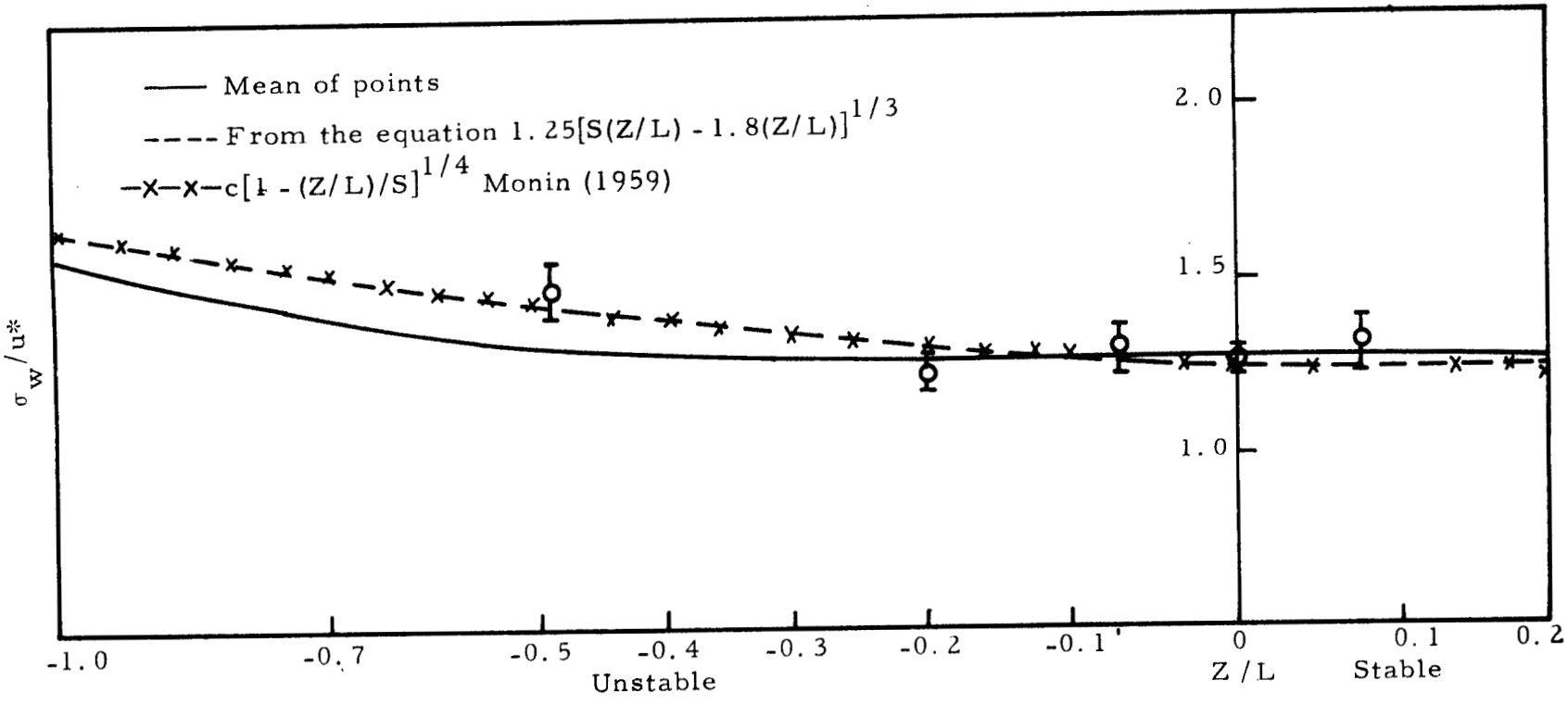

Figure 7. The Ratio of σ_w/u^* as a Function of Z/L According to Many Sources. Confidence Intervals Represent Standard Deviation of Means, Assuming all Observations are Independent of Each Other. (From Panofsky et al. [3])

$$B = \frac{RiS^2}{\ell n\left(\frac{Z}{Z_o}\right) - \Psi\left(\frac{Z}{L}\right)} \qquad (9)$$

where the parameters are as defined previously. Prasad and Panofsky show the relationship between σ_u/u^* and B in Figure 8. In neutral stability, $Z/L = 0$, $B = 0$, and $\sigma_u/u^* = 2.5$. The variation of σ_u/u^* with B is small, especially when compared with the lateral component. Although not immediately obvious by examination of Figure 8, other parameters constant, the variation of σ_u/u^* with Z/L is also small. Other investigations have found the same type of variation in σ_u/u^* with stability and height as Prasad and Panofsky. Since Prasad and Panofsky's work encompasses a wide variation in stability conditions and provides mathematical expressions for calculating σ_u, it has been chosen for inclusion in this model.

Lateral Standard Deviation - The lateral component standard deviation of gust velocity, like the longitudinal component, does not obey similarity theory. The ratio of σ_v/u^* in neutral stability has been found to vary from 1.3 to 2.6, depending not only upon surface roughness, Z_o, but apparently also upon the large scale terrain features. [15] The author knows of no mathematical expression that relates σ_v/u^* to Z_o and large scale roughness in neutral stability. Hence, an approximate value of $\sigma_v/u^* = 2.0$ in neutral stability will be used. The variation of σ_v/u^* with stability is much greater than for the longitudinal components. Prasad and Panofsky show the variation of σ_v/u^* with B in Figure 9. At $Z/L = 0$, $B = 0$, and $\sigma_v/u^* = 2.0$. Percentagewise, the variation of σ_v/u^* with stability is large, particularly in the unstable condition. Other investigators agree in general with Prasad and Panofsky's model[5]

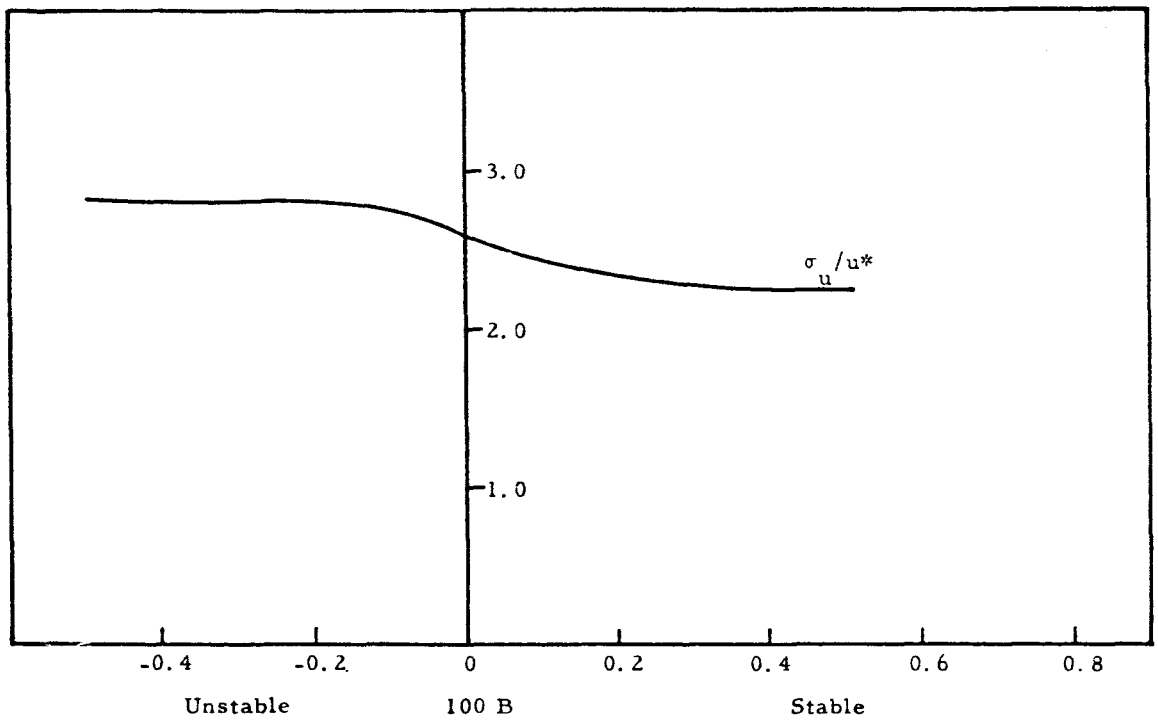

Figure 8. The Ratio σ_u/u^* as a Function of B at Many Sites. (From Panofsky et al. [3])

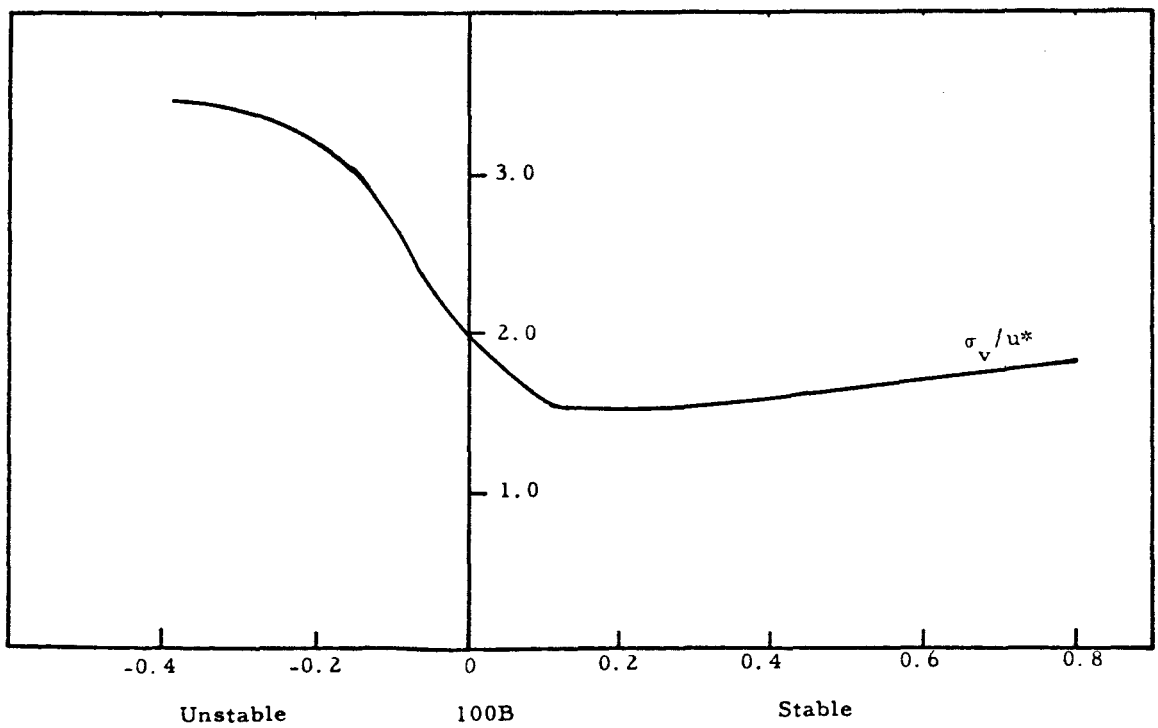

Figure 9. The ratio σ_v/u^* as a Function of B at Many Sites. (From Panofsky et al. [3])

Turbulence Spectra Scale Length

Vertical, longitudinal, and lateral components of scale length can be measured independently from experimental data. Physical laws, however, may demand an interrelationship between the various components. For example, in the free atmosphere, above the boundary layer, it is reasonable to apply the isotropic constraints $\sigma_u = \sigma_v = \sigma_w$ and $L_u = 2L_v = 2L_w$. In the surface boundary layer, total isotropy is certainly not valid, but local isotropy, or isotropy at high frequencies, is a tenable assumption. Total isotropy implies that the relationship

$$\Phi_w(K) = \frac{1}{2}\Phi_u - \frac{K}{2}\frac{\partial \Phi_u}{\partial K} = \Phi_v(K) \tag{10}$$

holds for all wave numbers K. For local isotropy, we will only require that Equation (10) hold for large wave numbers; that is, as $K \to \infty$. The longitudinal, vertical, and lateral spectral functions for the Dryden spectrum are

$$\Phi_u = \frac{4\sigma_u^2 L_u}{1 + (2\pi L_u K)^2}, \tag{11}$$

$$\Phi_w = \frac{4\sigma_w^2 L_w [1 + 3(4\pi L_w K)^2]}{[1 + (4\pi L_w K)^2]^2}, \tag{12}$$

and

$$\Phi_v = \frac{4\sigma_v^2 L_v [1 + 3(4\pi L_v K)^2]}{[1 + (4\pi L_v K)^2]^2}. \tag{13}$$

Substituting Equations (11), (12), and (13) into Equation (10) and letting $K \to \infty$ yields the relationship for local isotropy

$$\frac{L_u}{\sigma_u^2} = \frac{2L_w}{\sigma_w^2} = \frac{2L_v}{\sigma_v^2} \tag{14}$$

Having already described σ_u, σ_w, and σ_v for the surface boundary layer, it is only necessary to specify one component of L and then apply Equation (14) to define the other two components of scale length.

Vertical Scale Length - The vertical component of scale length can best be described independent of the local isotropy constraint for two reasons: (a) a large amount of experimental data exists concerning the vertical scale length, and (b) the conformance of the vertical component of turbulence to similarity theory implies a linear relationship of vertical scale length to height.

The vertical scale component is affected by the large scale terrain features. The surface roughness length may have some influence on L_w, but the nonuniformities and large scale features predominate. For neutral air over relatively flat terrain, a number of experimental results are available. Figure 10, extracted from Teunissen[10], shows results from several investigators. Teunissen summarizes their results and finds the relationship

$$L_w = 0.4\ Z \tag{15}$$

to provide a reasonable fit to the combined set of data. Sufficient results are not available to determine how the proportionality constant of Equation (15) varies over different types of terrain.

The variation of the vertical scale length with stability has been examined by Busch and Panofsky. [3] Busch and Panofsky find that the nondimensional frequency at which the normalized spectrum takes on its maximum value is related to stability by the expression

$$f_{max} = K_{max} Z = 0.32 \Phi_\epsilon (Z/L) \tag{16}$$

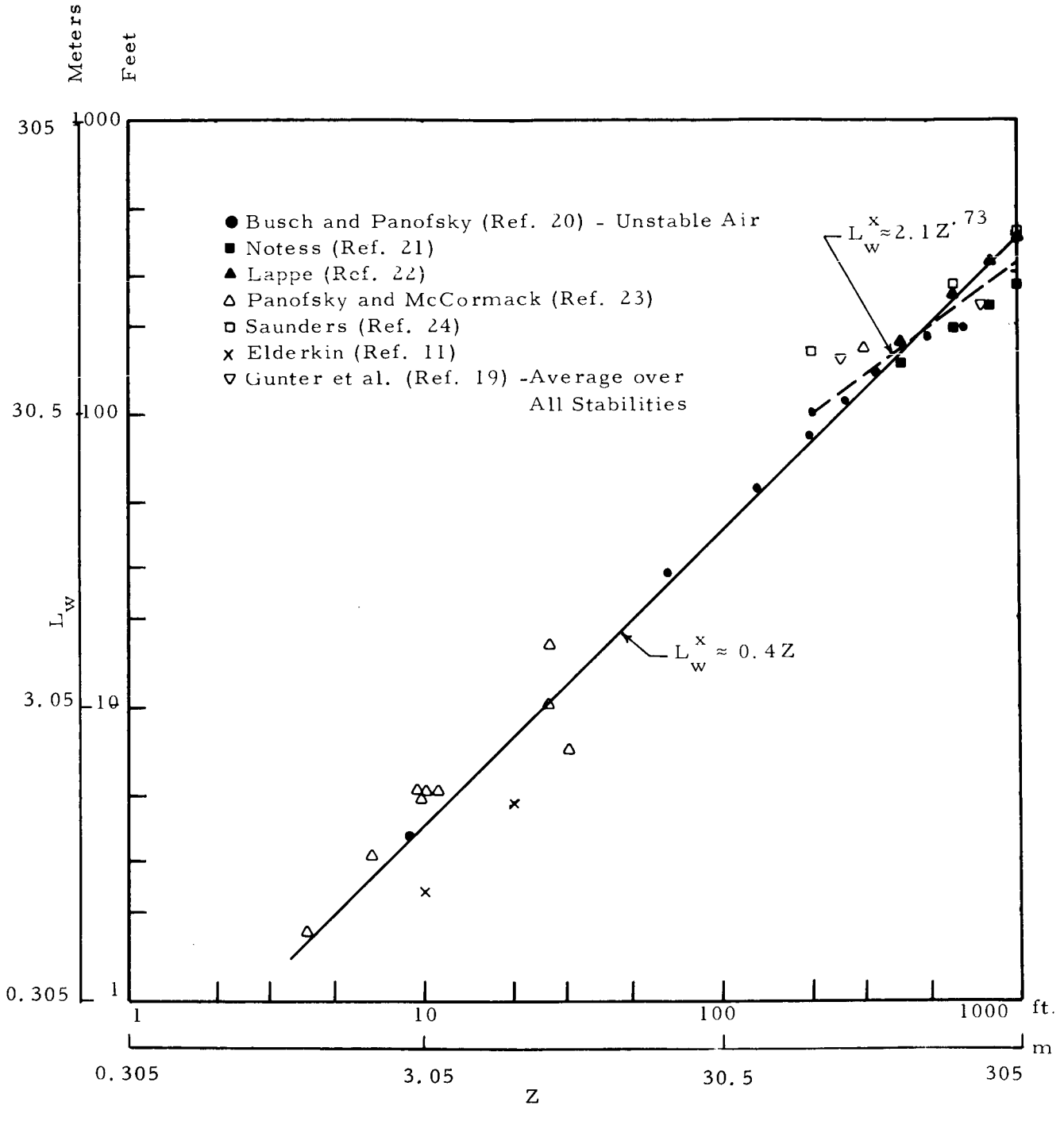

Figure 10. Vertical Component Scale Variation with Height in Neutral Stability over Flat Terrain (From Teunissen[10]).

where

$\Phi_\epsilon (Z/L)$ is the dimensionless dissipation rate.

For the Dryden spectrum, the vertical scale length, L_w, is related to the wave number where the normalized spectrum is a maximum by the equation

$$L_w = 0.117/K_{max}$$

or

$$L_w = \frac{0.117/Z}{f_{max}} \quad . \tag{17}$$

A substitution of Equation (16) into Equaton (17) gives

$$L_w = \frac{0.37Z}{\Phi\epsilon} \quad .$$

An analysis of several sets of data by Busch and Panofsky has provided the solid curve shown in Figure 11 (obtained from Reference 3) as representing the nondimensional dissipation rate Φ_ϵ. Two hypotheses have been suggested that postulate a balancing of the dissipation rate with other forces. They are

$$\Phi_\epsilon = S \tag{18a}$$

and

$$\Phi_\epsilon = S - \frac{Z}{L} \quad ; \tag{18b}$$

that is,

(a) dissipation rate equals mechanical energy production

and

(b) dissipation rate equals mechanical plus buoyant production.

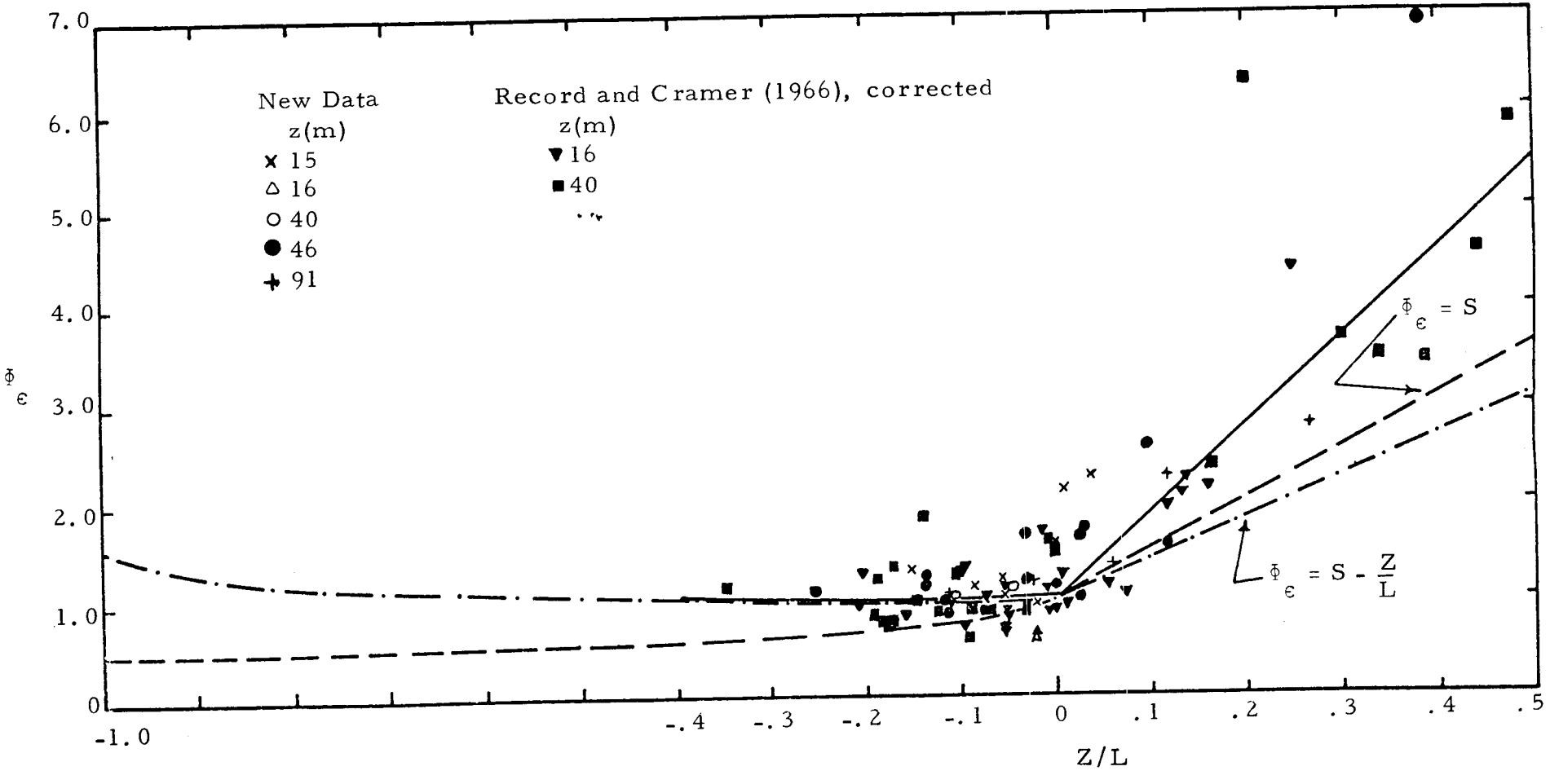

Figure 11. Normalized Dissipation at Round Hill as a Function of Z/L. Solid Line: Total Normalized Energy Production Obtained from Measurements at Equilibrium Sites. (From Panofsky et al. [3])

Figure 11 also compares Busch and Panofsky's curve to Equation (18a) and (18b) for S defined by Equations (4) and (5). On the stable side, neither assumption $\Phi_\epsilon = S$ or $\Phi_\epsilon = S - \frac{Z}{L}$ fits the data. Busch and Panofksy's solid line is derived from McVehil's [4] nondimensional shear expression of $S = 1 + 10\frac{Z}{L}$ and Equation (18b). This expression for the nondimensional shear is inconsistent with recent findings by Webb [2] and Businger et al. [6] Consequently, on the stable side we will choose Busch and Panofsky's function

$$\Phi_\epsilon = 1 + 9\frac{Z}{L} \tag{19}$$

for the dissipation rate because it empirically fits the data, while rejecting both balancing assumptions (18a) and (18b).

On the unstable side the dissipation rate appears balanced by the sum of the mechanical and bouyant energy production, at least to $Z/L = -0.4$. In strong instability sufficient data is not available for analysis. The function

$$\Phi_\epsilon = S - \frac{Z}{L} = (1-18\frac{Z}{L})^{-1/4} - \frac{Z}{L} \tag{20}$$

is used in the model to express the dissipation rate for the unstable condition.

The expression for the vertical scale length is obtained by substituting Equations (19) and (20) into Equation (17). This gives

$$L_w = \frac{0.37}{1 + 9\frac{Z}{L}} \qquad \text{for } \frac{Z}{L} \geq 0$$

and (21)

$$L_w = \frac{0.37}{(1-18\frac{Z}{L})^{-1/4} - \frac{Z}{L}} \quad \text{for } \frac{Z}{L} \leq 0.$$

In neutral stability, when $Z/L = 0$, Equations (21) reduce to $L_w = 0.37Z$ which is in good agreement with the proportionality constant of 0.4 recommended by Teunissen.

Longitudinal Scale Length - The longitudinal scale length is derived from the vertical and longitudinal standard deviations and the vertical scale length using the local isotropy relationship

$$\frac{L_u}{\sigma_u^2} = \frac{2L_w}{\sigma_w^2} \tag{14}$$

A comparison can be made in neutral stability to determine how well the values of L_u derived from Equation (14) compare with experimental measurements. In neutral stability the solution to Equation (14) for L_u gives

$$L_u = 2.96Z \quad .$$

Figure 12, from Teunissen[10], compares the line $L_u = 2.96Z$ with various experimental results. Although the line could not be considered an excellent fit, it does reasonably express the variation of L_u with stability, particulary above three-meter altitude.

Lateral Scale Length - As in the case of the longitudinal scale length, the lateral scale length is derived from the local isotropic relationship

$$\frac{L_v}{\sigma_v^2} = \frac{2L_w}{\sigma_w^2} \quad .$$

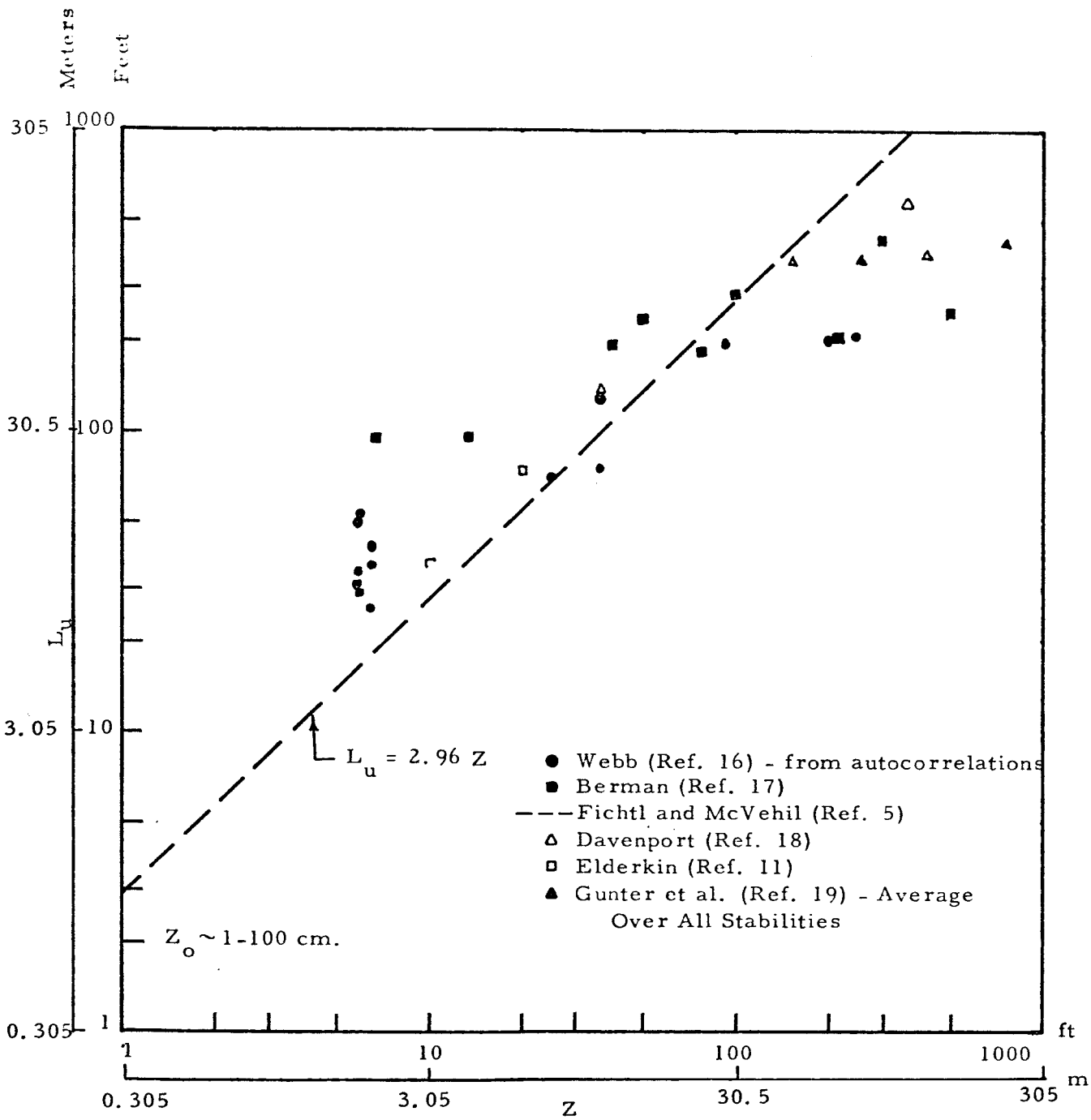

Figure 12. Longitudianl Component Scale Variation with Height in Neutral Stability over Flat Terrain (From Teunissen[10]).

In neutral stability, the solution to the above equation is

$$L_v = 1.89Z. \tag{22}$$

Figure 13 compares Equation (22) to the relationship found by Fichtl and McVehil in neutral air between 18 and 150 meters. The slope of the two curves disagrees considerably even though they pass through the same value at approximately 40 meters. Little other data is available from which to draw conclusions.

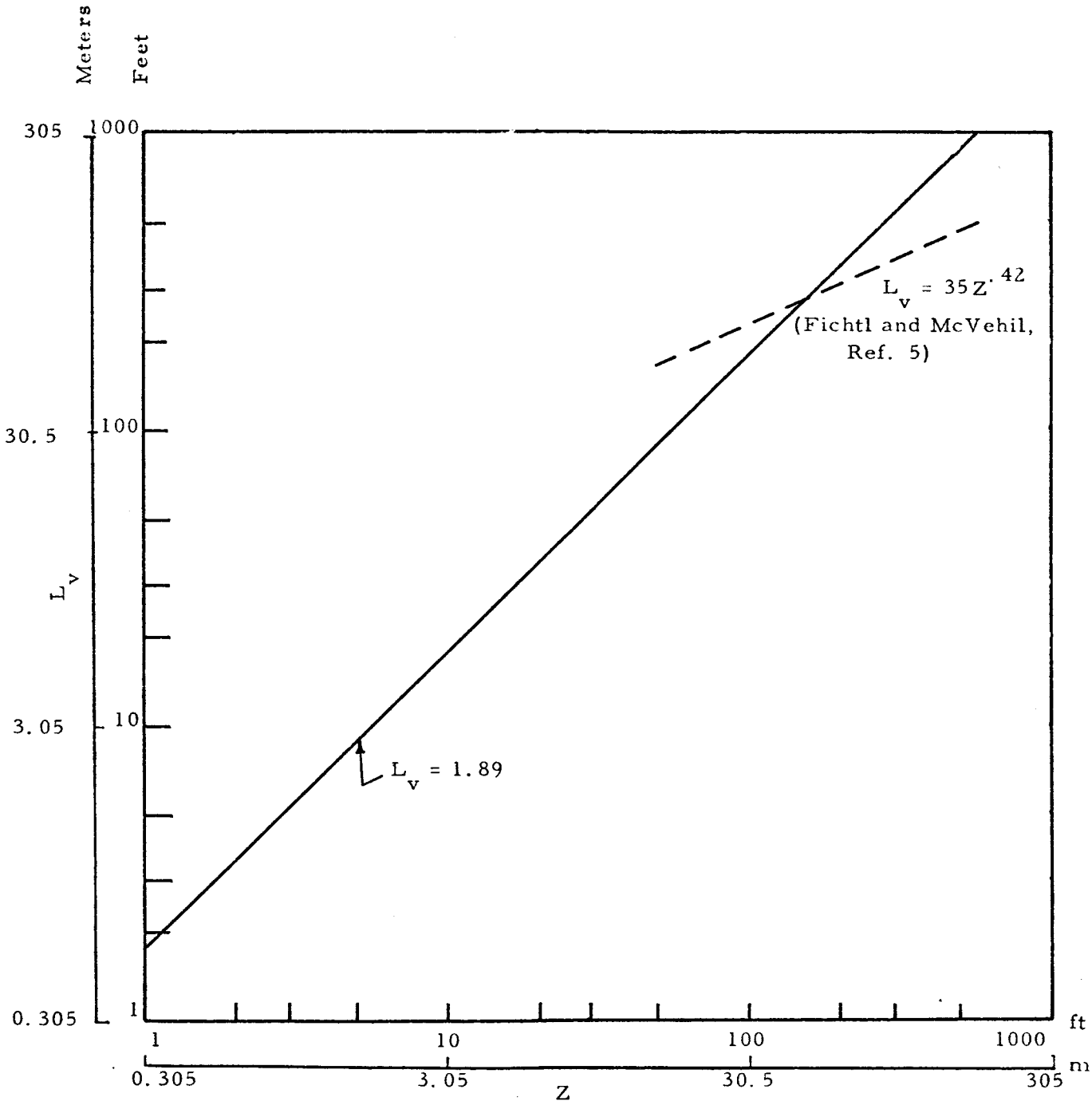

Figure 13. Lateral Component Scale Variation with Height in Neutral Stability.

REFERENCES

1. Fichtl, G. H., "Wind Shear Near the Ground and Aircraft Operations," Journal of Aircraft, November 1972.

2. Webb, E.K., "Profile Relationships: The Log-Linear Range, and Extension to Strong Stability," Quarterly Journal of the Royal Meteorological Society, Volume 96, 1970.

3. Panofsky, H.A., et al., "Properties of Wind and Temperature at Round Hill, Sought Dartmouth, Massachusetts," Research and Development Technical Report ECOM-0035-F, August 1967.

4. McVehil, G.E., "Wind and Temperature Profiles Near the Ground in Stable Stratification," Quarterly Journal of the Royal Meteorological Society, Volume 90, 1964.

5. Fichtl, G.H., and G.E. McVehil, "Longitudinal and Lateral Spectra of Turbulence in the Atmospheric Boundary Layer," NASA Technical Note NASA TN D-5584, February 1970.

6. Wyngaard, J.C., and O.R. Cote, "The Budgets of Turbulent Kinetic Energy and Temperature Variance in the Atmospheric Surface Layer," Journal of the Atmospheric Sciences, Volume 28, 1971.

7. Businger, J.A., J.C. Wyngaard, Y. Izumi, and E.F. Bradley, "Flux-Profil Relationships in the Atmospheric Surface Layer," Journal of the Atmospheric Sciences, Volume 28, March 1971.

8. Pettitt, R.B., and R.G. Root, "Vertical Wind Shear in the Boundary Layer," in World Meteorological Organization Technical Note No. 93, Geneva, Switzerland, 1969.

9. Flinn, E.H., "Low Altitude Turbulence and V/STOL Gust Response," AFFDL/FGC-TM-70-3, September 1970.

10. Teunissen, H.W., "Characteristics of the Mean Wind and Turbulence in the Planetary Boundary Layer," Institute for Aerospace Studies, University of Toronto, UTIAS Review No. 32, October 1970.

11. Elderkin, G.E., "Experimental Investigation of the Turbulence Structure in the Lower Atmosphere," Batelle-Northwest Report 329, Pacific N.W. Laboratory, Richland, Washington, December 1966.

12. Kaimal, J.C., and Y. Izumi, "Vertical Velocity Fluctuations in a Nocturnal Low-Level Jet," Journal of Applied Meteorology, Volume 4, Number 5, October 1965.

13. Mordukhovich, M., and L. Tsuang, USSR, Atmospheric and Ocean Physics 2, 1966.

14. Lumley, J.L., and H.A. Panofsky, The Structure of Atmospheric Turbulence, Interscience Publishers, 1964.

15. Pasquill, F., "Wind Structure in the Atmospheric Boundary Layer," Philosophical Transactions of the Royal Society of London, Series A, Volume 269, 1971.

16. Webb, E.K., "Autocorrelations and Energy Spectra of Atmospheric Tubulence," C.S.I.R.O., Australian Division of Meteorological Physics, Technical Paper Number 5, Melbourne, Australia, 1955.

17. Berman, S., "Estimating the Longitudinal Wind Spectrum Near the Ground," Quarterly Journal of the Royal Meteorological Society, Volume 91, 1965.

18. Davenport, A.G., "The Spectrum of Horizontal Gustiness Near the Ground in High Winds," Quarterly Journal of the Royal Meteorological Society, Volume 87, 1961.

19. Gunter, D.E., et al., "Low Altitude Atmospheric Turbulence, Lo-Locat, Phases I and II," ASD-TR-69-12, February 1969.

20. Busch, N., and H. Panofsky, "Recent Spectra of Atmospheric Turbulence," Proceedings of the Unguided Rocket Ballistic Meteorological Conference, New Mexico State University, 1967.

21. Notess, C., "Analysis of Turbulence Data Measured in Flight at Altitudes up to 1600 Feet above Three Different Types of Terrain," Cornell Aeronautical Labs, TE-1215-F-1, April 1959.

22. Lappe, U., "A Low Altitude Gust Model for Estimating Gust Loads on Aircraft," AIAA Paper 65-14, January 1965.

23. Panofsky, H., and R. McCormack, "The Spectrum of Vertical Velocity Near the Surface," IAS No. 59-6, January 1959.

24. Saunders, K., "B-66B Low Level Gust Study Volume I," WADD Technical Report 60-305, Wright-Patterson Air Force Base, Ohio, March 1961.